

Chiral three-nucleon force at N⁴LO I: Longest-range contributions

H. Krebs,^{1,*} A. Gasparyan,^{1,2,†} and E. Epelbaum^{1,‡}

¹*Institut für Theoretische Physik II, Ruhr-Universität Bochum, D-44780 Bochum, Germany*

²*SSC RF ITEP, Bolshaya Cheremushkinskaya 25, 117218 Moscow, Russia*

(Dated: October 30, 2018)

We derive the sub-subleading two-pion exchange contributions to the three-nucleon force which appear at next-to-next-to-next-to-next-to-leading order in chiral effective field theory. In order to determine the low-energy constants, a complete analysis of pion-nucleon scattering at the subleading-loop order in the heavy-baryon expansion is carried out utilizing the power counting scheme employed in the derivation of the nuclear forces. We discuss the convergence of the chiral expansion for this particular three-nucleon force topology and give the values of the low-energy constants which provide the most realistic description of the three-nucleon force when the chiral expansion is truncated at next-to-next-to-leading order.

PACS numbers: 13.75.Cs, 21.30.-x

I. INTRODUCTION

Three-nucleon forces (3NFs) are well known to play an important role in nuclear physics. In spite of many decades of effort, the detailed structure of the 3NF is not properly reproduced by modern phenomenological 3NF models, see Ref. [1] for a comprehensive review. This provides a strong motivation to explore the structure of the 3NF within chiral effective field theory (EFT) which is nowadays a standard tool to analyze low-energy nuclear dynamics in harmony with the symmetries of QCD, see Refs. [2–4] for recent review articles. In the past two decades, nuclear forces have already been extensively studied in this framework. For two nucleons, it turned out to be necessary and sufficient to go to next-to-next-to-next-to-leading order (N³LO) in order to accurately describe the static deuteron properties as well as the two-nucleon phase shifts and mixing angles up to laboratory energies of $E_{\text{lab}} \sim 200$ MeV [5, 6]. On the other hand, three- and more-nucleon systems are so far only analyzed up to next-to-next-to-leading order (N²LO) in the chiral expansion [7, 8]. At this order one gets the first non-vanishing contributions to the 3NF which emerge from the two-pion-exchange, one-pion-exchange-contact and purely contact graphs (a), (d) and (f) in Fig. 1 with the corresponding amplitudes being given by the lowest-order pion-nucleon vertices. Generally, one observes a good description of nucleon-deuteron elastic and breakup scattering observables at very low energies which improves when going from next-to-leading order (NLO) to N²LO. On the other hand, the well-known puzzles in the three-nucleon continuum such as e.g. the A_y -puzzle [9–11] and the large discrepancy for the breakup cross section in the so-called space-star and related configurations [12, 13] still persist at N²LO. Notice, however, that the recent calculation by the Pisa group [14] demonstrates that the A_y -puzzle in the 4N system is significantly reduced by the chiral 3NF at N²LO. The chiral EFT predictions for the three-nucleon scattering observables at N²LO at intermediate and higher energies are, in general, in agreement with the data but show a rapidly increasing theoretical uncertainty. It is, therefore, necessary to go to higher orders in the chiral expansion for three- and more-nucleon systems.

The N³LO contributions to the 3NF emerge from the leading relativistic corrections and pion-loop diagrams in all six topologies shown in Fig. 1. It is important to stress that the N³LO contributions do not involve any unknown low-energy constants (LECs). The corresponding parameter-free expressions can be found in Refs. [15, 16], see also Ref. [17]. Another interesting feature of the N³LO 3NF corrections is their rather rich isospin-spin-momentum structure emerging, especially, from the ring topology (c) in Fig. 1. This is in contrast with the quite restricted operator structure of the two-pion exchange 3NF topology (a) whose effects in the three-nucleon continuum have already been

*Email: hermann.krebs@rub.de

†Email: ashotg@tp2.rub.de

‡Email: evgeny.epelbaum@rub.de

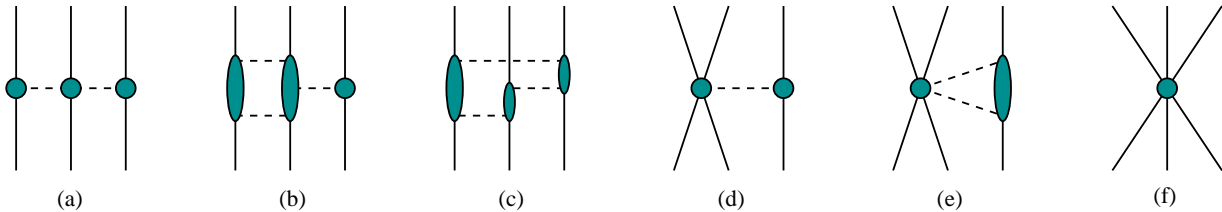


FIG. 1: Various topologies contributing to the 3NF up to and including $N^4\text{LO}$: two-pion (2π) exchange (a), two-pion-one-pion (2π - 1π) exchange (b), ring (c), one-pion-exchange-contact (d), two-pion-exchange-contact (e) and purely contact (f) diagrams. Solid and dashed lines represent nucleons and pions, respectively. Shaded blobs represent the corresponding amplitudes.

extensively explored. It is, therefore, very interesting to study the impact of the novel structures in the 3NF on nucleon-deuteron scattering and the properties of light nuclei, especially in connection with the already mentioned unsolved puzzles. On the other hand, one may ask whether the resulting (leading) contributions to the structure functions accompanying the novel operator structures in the 3NF already allow for their decent description. Stated differently, the question is whether the lowest-nonvanishing-order contributions from the 2π - 1π and ring-topologies are already converged or, at least, provide a reasonable approximation to the converged result. There is a strong reason to believe that this is not going to be the case since the contributions due to intermediate $\Delta(1232)$ excitations are not yet taken into account for these topologies at $N^3\text{LO}$. In the standard chiral EFT formulation based on pions and nucleons as the only explicit degrees of freedom, effects of the Δ (and heavier resonances as well as heavy mesons) are hidden in the (renormalized) values of certain LECs starting from the subleading effective Lagrangian. The major part of the Δ contributions to the nuclear forces is taken into account in the Δ -less theory through resonance saturation of the LECs $c_{3,4}$ accompanying the subleading $\pi\pi NN$ vertices [18–22] (see, however, the last two references for some examples of the Δ -contributions that go beyond the saturation of $c_{3,4}$). These LECs turn out to be numerically large and are known to be driven by the Δ isobar [20, 23]. As a consequence, one observes a rather unnatural convergence pattern in the chiral expansion of the two-pion exchange nucleon-nucleon potential $V_{NN}^{2\pi}$ with by far the strongest contribution resulting from the formally subleading triangle diagram proportional to c_3 [24]. The (formally) leading contribution to $V_{NN}^{2\pi}$ does not provide a good approximation to the potential so that one needs to go to (at least) the next-higher order in the chiral expansion and/or to include the Δ isobar as an explicit degree of freedom [20]. The situation with the 2π - 1π and ring topologies in the 3NF is similar. Based on the experience with the two-nucleon potential, one expects significant contributions due to intermediate Δ excitations, see also the discussion in Ref. [25]. For the ring topology, this expectation is confirmed by the phenomenological study of Ref. [26]. In order to include effects of the Δ -isobar one needs

- either to go to (at least) next-to-next-to-next-to-next-to-leading order ($N^4\text{LO}$) in the standard Δ -less EFT approach
- or to include the Δ -isobar as an explicit degree of freedom.

It should be understood that both strategies outlined above are, to some extent, complementary to each other. In particular, $N^3\text{LO}$ contributions in the Δ -less theory only take into account effects due to single Δ -excitation but not due to the double and triple Δ -excitations (whose inclusion in the Δ -less approach would require the calculation at even higher orders). These effects are taken into account already at $N^3\text{LO}$ in the Δ -full approach. On the other hand, there are also contributions not related to Δ -excitations which are included/absent in the Δ -less approach at $N^4\text{LO}/\Delta$ -full theory at $N^3\text{LO}$. It remains to be seen which strategy will turn out to be most efficient. The present paper represents the first step along this line. We analyze here the longest-range contribution to the 3NF in the standard, Δ -less approach at $N^4\text{LO}$ in the chiral expansion. This topology is particularly challenging due to (i) the need to carry out a non-trivial renormalization program as explained in section III and (ii) the need to re-consider pion-nucleon scattering in order to determine the relevant LECs. Our paper is organized as follows. In section II, we specify all terms in the effective Lagrangian that are needed in the calculation. The general structure of the two-pion exchange 3NF is discussed in section III. Here, we also briefly summarize the already available results at $N^2\text{LO}$ and $N^3\text{LO}$ and give explicit expressions for the $N^4\text{LO}$ contributions. In section IV we analyze pion-nucleon scattering at order Q^4 in the chiral expansion with Q referring to the soft scale of the order of the pion mass and use the available partial wave analyses to determine the relevant LECs. In section V, the numerical results for the two-pion exchange

3NF are presented and the convergence of the chiral expansion is discussed. Finally, the findings of our work are briefly summarized in section VI. The Appendices contain explicit formulae for the algebraic structure of the nuclear Hamiltonian at order N⁴LO and the chiral expansion of the πN invariant amplitudes.

II. EFFECTIVE LAGRANGIAN

To derive the longest-range contributions to the 3NF at N⁴LO we need the effective pion-nucleon Lagrangian up to the order Q^4 . The explicit expressions in the heavy-baryon formulation can be found in Ref. [27, 28]. For the sake of completeness, we list here all terms relevant for our calculation with the corresponding building blocks being expanded in powers of the pion fields:

$$\begin{aligned}
\mathcal{L}_{\pi N}^{(1)} &= N_v^\dagger \left[iv \cdot \partial - \frac{1}{4F^2} \boldsymbol{\tau} \times \boldsymbol{\pi} \cdot (v \cdot \partial \boldsymbol{\pi}) + \frac{8\alpha - 1}{16F^4} \boldsymbol{\pi} \cdot \boldsymbol{\pi} \boldsymbol{\tau} \times \boldsymbol{\pi} \cdot (v \cdot \partial \boldsymbol{\pi}) \right. \\
&\quad \left. - \frac{\hat{g}_A}{F} \boldsymbol{\tau} \cdot (S \cdot \partial \boldsymbol{\pi}) + \frac{\hat{g}_A}{2F^3} ((4\alpha - 1) \boldsymbol{\tau} \cdot \boldsymbol{\pi} \boldsymbol{\pi} \cdot (S \cdot \partial \boldsymbol{\pi}) + 2\alpha \boldsymbol{\pi}^2 \boldsymbol{\tau} \cdot (S \cdot \partial \boldsymbol{\pi})) \right] N_v + \dots, \\
\mathcal{L}_{\pi N}^{(2)} &= N_v^\dagger \left[4M^2 c_1 - \frac{2}{F^2} c_1 M^2 \boldsymbol{\pi}^2 + \frac{1}{F^2} \left(c_2 - \frac{g_A^2}{8m} \right) (v \cdot \partial \boldsymbol{\pi}) \cdot (v \cdot \partial \boldsymbol{\pi}) + \frac{1}{F^2} c_3 (\partial_\mu \boldsymbol{\pi}) \cdot (\partial^\mu \boldsymbol{\pi}) \right. \\
&\quad - \frac{i}{F^2} \left(c_4 + \frac{1}{4m} \right) [S_\mu, S_\nu] \boldsymbol{\tau} \times (\partial^\nu \boldsymbol{\pi}) \cdot (\partial^\mu \boldsymbol{\pi}) + \frac{M^2 c_1}{2F^4} (8\alpha - 1) (\boldsymbol{\pi} \cdot \boldsymbol{\pi})^2 + \frac{c_3}{F^4} ((1 - 4\alpha) \boldsymbol{\pi} \cdot \partial_\mu \boldsymbol{\pi} \boldsymbol{\pi} \cdot \partial^\mu \boldsymbol{\pi} \\
&\quad - 2\alpha \boldsymbol{\pi} \cdot \boldsymbol{\pi} \partial_\mu \boldsymbol{\pi} \cdot \partial^\mu \boldsymbol{\pi}) - \frac{i c_4}{2F^4} (2(1 - 4\alpha) \boldsymbol{\tau} \cdot (\boldsymbol{\pi} \times \partial_\mu \boldsymbol{\pi}) \boldsymbol{\pi} \cdot \partial_\nu \boldsymbol{\pi} - 4\alpha \boldsymbol{\pi} \cdot \boldsymbol{\pi} \partial_\mu \boldsymbol{\pi} \cdot (\boldsymbol{\tau} \times \partial_\nu \boldsymbol{\pi})) [S^\mu, S^\nu] + \frac{\vec{\nabla}^2}{2m} \\
&\quad \left. + \frac{i \hat{g}_A}{2Fm} \left(\boldsymbol{\tau} \cdot (v \cdot \partial S \cdot \partial \boldsymbol{\pi}) + 2\boldsymbol{\tau} \cdot (v \cdot \partial \boldsymbol{\pi}) S \cdot \partial \right) + \frac{i}{8F^2 m} \left(\boldsymbol{\tau} \cdot (\boldsymbol{\pi} \times (\vec{\nabla}^2 \boldsymbol{\pi})) + \boldsymbol{\tau} \cdot (\boldsymbol{\pi} \times \vec{\nabla} \boldsymbol{\pi}) \vec{\nabla} \right) \right] N_v + \dots, \\
\mathcal{L}_{\pi N}^{(3)} &= N_v^\dagger \left[\frac{2}{F^2} \left(d_1 + d_2 - \frac{c_4}{4m} \right) \boldsymbol{\tau} \times (\partial_\mu v \cdot \partial \boldsymbol{\pi}) \cdot (\partial^\mu \boldsymbol{\pi}) + \frac{2}{F^2} d_3 \boldsymbol{\tau} \times ((v \cdot \partial)^2 \boldsymbol{\pi}) \cdot (v \cdot \partial \boldsymbol{\pi}) - \frac{4}{F^2} d_5 M^2 \boldsymbol{\tau} \times \boldsymbol{\pi} \cdot (v \cdot \partial \boldsymbol{\pi}) \right. \\
&\quad - \frac{2i}{F^2} (d_{14} - d_{15}) [(S \cdot \partial v \cdot \partial \boldsymbol{\pi}), (S \cdot \partial \boldsymbol{\pi})] - \frac{2}{F} (2d_{16} - d_{18}) M^2 \boldsymbol{\tau} \cdot (S \cdot \partial \boldsymbol{\pi}) \\
&\quad + \frac{i c_2}{F^2 m} \left((v \cdot \partial \boldsymbol{\pi}) \cdot (\partial_\mu \boldsymbol{\pi}) \vec{\partial}^\mu - \overleftarrow{\partial}^\mu (v \cdot \partial \boldsymbol{\pi}) \cdot (\partial_\mu \boldsymbol{\pi}) \right) - \frac{c_4}{2F^2 m} \left(\boldsymbol{\tau} \cdot ((v \cdot \partial \boldsymbol{\pi}) \times (\partial^2 \boldsymbol{\pi})) \right. \\
&\quad \left. - 2\boldsymbol{\tau} \cdot ((v \cdot \partial \boldsymbol{\pi}) \times (\partial_\mu \boldsymbol{\pi})) [S^\mu, S^\nu] \vec{\partial}_\nu + 2 \overleftarrow{\partial}_\nu \boldsymbol{\tau} \cdot ((v \cdot \partial \boldsymbol{\pi}) \times (\partial_\mu \boldsymbol{\pi})) [S^\mu, S^\nu] \right) \left. \right] N_v + \dots, \\
\mathcal{L}_{\pi N}^{(4)} &= N_v^\dagger \left[2(8e_{38} + e_{115} + e_{116}) M^4 - \frac{i}{F^2} [S_\mu, S_\nu] \left(-18e_{17} \boldsymbol{\tau} \times (\partial^\rho \partial^\mu \boldsymbol{\pi}) \cdot (\partial_\rho \partial^\nu \boldsymbol{\pi}) + e_{18} \boldsymbol{\tau} \times (v \cdot \partial \partial^\mu \boldsymbol{\pi}) \cdot (v \cdot \partial \partial^\nu \boldsymbol{\pi}) \right. \right. \\
&\quad + 4(2e_{21} - e_{37}) M^2 \boldsymbol{\tau} \times (\partial^\nu \boldsymbol{\pi}) \cdot (\partial^\mu \boldsymbol{\pi}) \left. \right) + 8e_{14} (\partial_\mu \partial_\nu \boldsymbol{\pi}) \cdot (\partial^\mu \partial^\nu \boldsymbol{\pi}) + 8e_{15} (v \cdot \partial \partial_\mu \boldsymbol{\pi}) \cdot (v \cdot \partial \partial^\mu \boldsymbol{\pi}) \\
&\quad + 8e_{16} ((v \cdot \partial)^2 \boldsymbol{\pi}) \cdot ((v \cdot \partial)^2 \boldsymbol{\pi}) + 4M^2 (2e_{19} - e_{22} - e_{36}) (\partial_\mu \boldsymbol{\pi}) \cdot (\partial^\mu \boldsymbol{\pi}) + 8e_{20} M^2 (v \cdot \partial \boldsymbol{\pi}) \cdot (v \cdot \partial \boldsymbol{\pi}) \\
&\quad \left. - 4e_{22} M^2 \boldsymbol{\pi} \cdot (\partial_\mu \partial^\mu \boldsymbol{\pi}) - 8e_{35} M^2 \boldsymbol{\pi} \cdot ((v \cdot \partial)^2 \boldsymbol{\pi}) - 16e_{38} M^4 \boldsymbol{\pi}^2 \right] N_v + \dots, \tag{2.1}
\end{aligned}$$

where $\boldsymbol{\pi}$ and N_v refer to pion and nucleon fields, $\boldsymbol{\tau}$ denote the isospin Pauli matrices, v is the nucleon four-velocity and S_μ refers to the covariant spin operator of the nucleon,

$$S_\mu = \frac{1}{2} i \gamma_5 \sigma_{\mu\nu} v^\nu, \quad \sigma_{\mu\nu} = \frac{i}{2} [\gamma_\mu, \gamma_\nu]. \tag{2.2}$$

Further, F and \hat{g}_A are the pion decay and the nucleon axial vector constants in the chiral limit, M is the pion mass to leading order in quark masses and d_i (e_i) are further low-energy constants (LECs) from the order- Q^3 (order- Q^4) pion-nucleon Lagrangian. The superscript i of $\mathcal{L}_{\pi N}^{(i)}$ refers to the number of derivatives or insertions of the pion mass. Notice that in the power counting scheme employed here, the nucleon mass is treated as a heavier scale as compared to the chiral-symmetry-breaking scale Λ_χ , see the discussion at the end of the section III B. As a consequence, the $1/m^2$ -terms in $\mathcal{L}_{\pi N}^{(3)}$ and the $1/m$ -, $1/m^2$ - and $1/m^3$ -terms in $\mathcal{L}_{\pi N}^{(4)}$ generate contributions to the 3NF beyond N⁴LO.

We, therefore, refrain from listing these terms in the effective Lagrangian. The constant α represents the freedom in parametrizing the pion field. Clearly, physical observables should not depend on a particular choice of α . Therefore, keeping α unspecified and verifying α -independence of the resulting nuclear forces allows for a non-trivial check of the calculation. Notice that isospin-breaking corrections to the 3NF start to contribute at N³LO. The complete expressions for isospin-breaking terms in the 3NF up to and including N⁴LO can be found in Ref. [29], see also [30, 31]. We, therefore, refrain from including isospin-breaking terms in the present work and employ exact isospin symmetry. For more details on the effective pion-nucleon Lagrangian the reader is referred to Refs. [28, 32, 33].

III. THE TWO-PION EXCHANGE 3NF

The 2π -exchange topology (a) generates the longest-range contribution to the 3NF. In the isospin and static limits, its general structure in momentum space has the following form (modulo terms of a shorter range such as e.g. the ones corresponding to the (b)-topology):

$$V_{2\pi} = \frac{\vec{\sigma}_1 \cdot \vec{q}_1 \vec{\sigma}_3 \cdot \vec{q}_3}{[q_1^2 + M_\pi^2][q_3^2 + M_\pi^2]} \left(\tau_1 \cdot \tau_3 \mathcal{A}(q_2) + \tau_1 \times \tau_3 \cdot \tau_2 \vec{q}_1 \times \vec{q}_3 \cdot \vec{\sigma}_2 \mathcal{B}(q_2) \right), \quad (3.3)$$

where $\vec{\sigma}_i$ denote the Pauli spin matrices for the nucleon i and $\vec{q}_i = \vec{p}_i' - \vec{p}_i$, with \vec{p}_i' and \vec{p}_i being the final and initial momenta of the nucleon i . Here and in what follows, we use the notation: $q_i \equiv |\vec{q}_i|$. The quantities $\mathcal{A}(q_2)$ and $\mathcal{B}(q_2)$ in Eq. (3.3) are scalar functions of the momentum transfer q_2 of the second nucleon whose explicit form is derived within the chiral expansion. Unless stated otherwise, the expressions for the 3NF results are always given for a particular choice of the nucleon labels. The complete result can then be found by taking into account all possible permutations of the nucleons

$$V_{3N}^{\text{full}} = V_{3N} + 5 \text{ permutations}. \quad (3.4)$$

It is important to emphasize that we are using in Eq. (3.3) a slightly different notation as compared to e.g. Ref. [15]. Specifically, in order to avoid the issue of non-uniqueness of a decomposition into the 2π , 2π - 1π and shorter-range contributions, we get rid of all terms which are proportional to q_1^2 and q_3^2 . More precisely, using the identity $q_{1,3}^2 = (q_{1,3}^2 + M_\pi^2) - M_\pi^2$ and canceling the inverse pion propagator with the corresponding one in Eq. (3.3), each $q_{1,3}^2$ in the numerator gets replaced by $-M_\pi^2$ modulo some additional contributions to the two-pion-one-pion exchange, one-pion-exchange-contact and the purely short-range contact interactions V_{cont} , see graphs (b), (d) and (f) in Fig. 1. This way we ensure that the resulting functions \mathcal{A} and \mathcal{B} depend solely on q_2 rather than on q_1 , q_2 and q_3 . The purely short-range, induced terms V_{cont} only shift the low-energy constants accompanying the contact 3NFs whose values anyway need to be adjusted to the data. There is no need to keep these contributions explicitly. The induced contributions to the other two topologies do, however, need to be taken into account, see Ref. [34] for a related discussion.

A. N²LO and N³LO contributions

We now briefly consider the first two terms in the chiral expansion of the functions $\mathcal{A}(q_2)$ and $\mathcal{B}(q_2)$. The leading contributions arise at N²LO which corresponds to the order Q^3 relative to the leading contribution to the nuclear Hamiltonian and have the form [7, 8]

$$\mathcal{A}^{(3)}(q_2) = \frac{g_A^2}{8F_\pi^4} \left((2c_3 - 4c_1)M_\pi^2 + c_3q_2^2 \right), \quad \mathcal{B}^{(3)}(q_2) = \frac{g_A^2 c_4}{8F_\pi^4}, \quad (3.5)$$

where g_A , F_π and M_π denote to the physical values of the nucleon axial vector coupling, pion decay constant and pion mass, respectively, and the superscripts of \mathcal{A} and \mathcal{B} refer to the powers of the soft scale Q . The first corrections at N³LO read [15, 17]:

$$\begin{aligned} \mathcal{A}^{(4)}(q_2) &= \frac{g_A^4}{256\pi F_\pi^6} \left[A(q_2) (2M_\pi^4 + 5M_\pi^2 q_2^2 + 2q_2^4) + (4g_A^2 + 1) M_\pi^3 + 2(g_A^2 + 1) M_\pi q_2^2 \right], \\ \mathcal{B}^{(4)}(q_2) &= -\frac{g_A^4}{256\pi F_\pi^6} \left[A(q_2) (4M_\pi^2 + q_2^2) + (2g_A^2 + 1) M_\pi \right], \end{aligned} \quad (3.6)$$

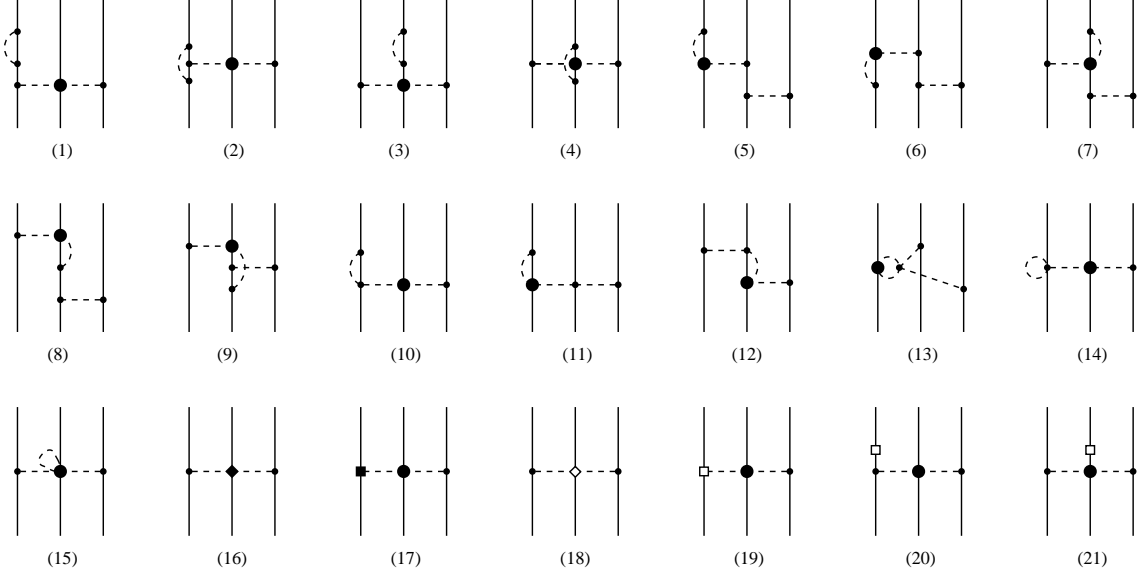


FIG. 2: Two-pion exchange 3N diagrams at $N^4\text{LO}$. Solid dots, filled circles, rectangles and diamonds denote vertices from $\mathcal{L}_{\pi N}^{(1)}$ or $\mathcal{L}_{\pi}^{(2)}$, $\mathcal{L}_{\pi N}^{(2)}$, $\mathcal{L}_{\pi N}^{(3)}$ or $\mathcal{L}_{\pi}^{(4)}$ and $\mathcal{L}_{\pi N}^{(4)}$, respectively. Open rectangles (diamonds) refer to $1/m$ -vertices from $\mathcal{L}_{\pi N}^{(2)}$ ($\mathcal{L}_{\pi N}^{(3)}$). Diagrams which result from the interchange of the nucleon lines and/or application of the time reversal operation are not shown. For remaining notation see Fig. 1.

where the loop function $A(q)$ is defined as:

$$A(q) = \frac{1}{2q} \arctan \frac{q}{2M_{\pi}}. \quad (3.7)$$

Notice that the leading-loop contributions to the 2π -exchange topology do not contain logarithmic ultraviolet divergences and, as explained in Ref. [15], turn out to be independent from the LECs d_i entering $\mathcal{L}_{\pi N}^{(3)}$. At both $N^2\text{LO}$ and $N^3\text{LO}$, all LECs in the effective Lagrangian entering the expressions for the 3NF – including g_A and F_{π} – can be simply replaced by their physical values.

We further emphasize that, as already mentioned above, the expressions in Eq. (3.6) differ from the ones in Eq. (2.9) of Ref. [15] by terms of a shorter range as compared to the two-pion exchange contributions. The advantage of using the new notation is that the results for \mathcal{A} and \mathcal{B} are now α -independent. This was not the case for terms in Eq. (2.9) of Ref. [15] where the results are given for a specific choice $\alpha = 0$.

Last but not least, we emphasize that relativistic corrections to $V_{2\pi}$ have a richer structure than the one given in Eq. (3.3). The explicit form of the $1/m$ -corrections to $V_{2\pi}$ at $N^3\text{LO}$ can be found in Ref. [16], see also [35] for an early work.

B. $N^4\text{LO}$ contributions

We now turn to the sub-subleading contributions to the 2π -exchange 3NF at order Q^5 ($N^4\text{LO}$). These are depicted in Fig. 2 and emerge from:

- one-loop diagrams (1)-(15) constructed from the leading-order vertices from $\mathcal{L}_{\pi N}^{(1)}$ and a single insertion of a subleading vertex $\propto c_i$,
- tree diagram (16) involving leading-order vertices from $\mathcal{L}_{\pi N}^{(1)}$ and a single insertion of a vertex from $\mathcal{L}_{\pi N}^{(4)}$ proportional to LECs e_i ,

- tree diagram (17) involving leading-order vertices from $\mathcal{L}_{\pi N}^{(1)}$, one $\mathcal{L}_{\pi N}^{(2)}$ -vertex $\propto c_i$ and one $\mathcal{L}_{\pi N}^{(3)}$ -vertex $\propto \bar{d}_i$,
- relativistic $1/m$ -corrections resulting from diagrams (18)-(21).

Notice that since we work with renormalized pion field operators, we do not show explicitly in Fig. 2 diagrams involving pion self energy. We further emphasize that some of the diagrams shown in Fig. 2, such as e.g. graphs (10) and (11), yield vanishing contributions to the 3NF.

It is important to keep in mind that, in order to derive the genuine 3NF contributions, we need to separate the irreducible parts in the corresponding amplitudes to avoid double counting when iterating the potentials in the scattering equation. This is achieved employing the method of unitary transformation, see Refs. [36, 37] for a comprehensive description of the method, Refs. [15, 16, 38, 39] for recent higher-order calculations of three- and four-nuclear forces and Refs. [40, 41] for an extension to electromagnetic processes. More precisely, we only use the method of unitary transformation to evaluate the contributions of graphs (1), (3), (5), (6)-(8), (20) and (21) in Fig. 1 which involve reducible topologies. The remaining contributions are obtained by calculating the corresponding Feynmann diagrams.

Before showing our results for the N^4 LO contributions to the functions \mathcal{A} and \mathcal{B} , we briefly remind the reader how the calculations within the method of unitary transformation are organized. We begin with the effective Lagrangian specified in section II and switch to the Hamiltonian using the canonical formalism. We prefer to work with renormalized pion field $\pi^r = Z_\pi^{-1/2} \pi$ and mass M_π and, therefore, do not need to deal with pion self-energy contributions. In the second step, the pion degrees of freedom are projected out by employing the appropriate unitary transformation in the Fock space. The explicit form of the unitary operator needed to compute nuclear forces up to N^3 LO can be found in Ref. [16, 39]. It is important to emphasize that getting rid of ultraviolet divergences appearing in the pion loop contributions to the nuclear Hamiltonian and current operators by expressing the bare LECs in terms of renormalized ones is not guaranteed a priori (given that the nuclear forces and currents are not observable quantities). This issue is discussed in detail in Ref. [39], see also Ref. [41]. To ensure renormalizability, we exploit the unitary ambiguity of the resulting nuclear potentials, i.e. the freedom in choosing the basis states in the Hilbert space. More precisely, we apply additional unitary transformations in the purely nucleonic subspace of the Fock space whose “rotation angles” are chosen in such a way, that all ultraviolet divergences are absorbed into redefinition of the LECs. As explicitly demonstrated in Refs. [39, 41], it is possible to carry out this renormalization program for the leading-loop contributions to the 3NF and the electromagnetic two-nucleon current operators. An extension to subleading-loop 3NF contributions at N^4 LO is straightforward. In Appendix A we show the resulting formal algebraic structure of the N^4 LO contributions to the nuclear force $\propto g_A^4 c_i$ and the retardation corrections $\propto g_A^2 c_i/m$. To evaluate the corresponding 3NF contributions, we simply compute the matrix elements of the connected time-ordered-like 3N diagrams emerging from these operators and employ dimensional regularization to deal with ultraviolet divergencies. The unitary ambiguity is parametrized via the “rotation angles” $\alpha_{9,10,11}$ which have to be chosen in such a way that the 3NF matrix elements become finite when expressed in terms of renormalized LECs. At the order we are working, the relations between the LECs \check{g}_A , F and M and the corresponding renormalized constants are given by

$$\begin{aligned}\check{g}_A &= g_A + \frac{g_A^3 M_\pi^2}{16\pi^2 F_\pi^2} - 4d_{16}M_\pi^2 + \frac{2g_A(2g_A^2 + 1)\lambda_\pi M_\pi^2}{F^2} + \frac{g_A(c_3 - 2c_4)M_\pi^3}{6\pi F_\pi^2} + \mathcal{O}(M_\pi^4, 1/m), \\ F &= F_\pi + \frac{M_\pi^2(2\lambda_\pi - l_4)}{F_\pi} + \mathcal{O}(M_\pi^4), \\ M^2 &= M_\pi^2 - \frac{M_\pi^4(2l_3 + \lambda_\pi)}{F_\pi^2} + \mathcal{O}(M_\pi^6),\end{aligned}\tag{3.8}$$

where $l_{3,4}$ are the LECs entering the subleading pion Lagrangian $\mathcal{L}_\pi^{(4)}$ [42] and the (divergent) quantity λ_π is defined, following the notation of Ref. [44], via

$$\lambda_\pi = \frac{M^{d-4}}{16\pi^2} \left[\frac{1}{d-4} - \frac{1}{2} (\Gamma'(1) + 1 + \log(4\pi)) \right].\tag{3.9}$$

We also need the expression for the pion Z -factor Z_π , which has the form

$$Z_\pi = 1 + \frac{2M_\pi^2}{F_\pi^2} ((10\alpha - 1)\lambda_\pi - l_4) + \mathcal{O}(M_\pi^4).\tag{3.10}$$

Notice that the Z -factor is not observable and shows an explicit dependence on α . For $\alpha = 0$, our result coincide with the one given in Ref. [44]. Further, the LECs l_i , d_i and e_i can be decomposed into the divergent parts and finite pieces. Utilizing the notation of Ref. [44]¹ this decomposition has the form:

$$\begin{aligned} l_i &= l_i^r(\mu) + \gamma_i \lambda = \frac{1}{16\pi^2} \bar{l}_i + \gamma_i \lambda_\pi, \\ d_i &= d_i^r(\mu) + \frac{\delta_i}{F^2} \lambda = \bar{d}_i + \frac{\delta_i}{F^2} \lambda_\pi, \\ e_i &= e_i^r(\mu) + \frac{\epsilon_i}{F^2} \lambda = \bar{e}_i + \frac{\epsilon_i}{F^2} \lambda_\pi, \end{aligned} \quad (3.11)$$

where μ denotes the renormalization scale and the divergent, μ -dependent quantity λ is related to the μ -independent one λ_π through

$$\lambda = \lambda_\pi - \frac{1}{32\pi^2} \log\left(\frac{M^2}{\mu^2}\right). \quad (3.12)$$

The coefficients γ_i and δ_i are well known in the framework of dimensional regularization adopted in the present work [32, 33, 42, 43]. The relevant coefficients read:

$$\delta_{18} = 0, \quad \delta_{16} = \frac{1}{2} \dot{g}_A + \dot{g}_A^3, \quad \gamma_3 = -\frac{1}{2}, \quad \gamma_4 = 2. \quad (3.13)$$

To the best of our knowledge, the ϵ_i -coefficients have not yet been worked out. Fortunately, we only need a few linear combinations of ϵ_i which are exactly the same as ones appearing in πN scattering at order Q^4 . Cancellation of the ultraviolet divergences in the πN scattering amplitude implies the following relations for the divergent parts of the LECs e_i [44]:

$$\begin{aligned} \epsilon_{14} &= -\frac{1}{12} c_2 - \frac{1}{2} c_3, \\ \epsilon_{17} &= -\frac{1}{12} c_4, \\ -2\epsilon_{19} + \epsilon_{22} + \epsilon_{36} &= -2c_1 + \frac{5}{24} c_2 - \frac{3}{4} c_3, \\ -2\epsilon_{21} + \epsilon_{37} &= -\frac{2}{3} c_4 - 3g_A^2 c_4, \\ \epsilon_{22} - 4\epsilon_{38} &= -3c_1 + \frac{1}{4} c_2 + \frac{3}{4} c_3. \end{aligned} \quad (3.14)$$

Expressing the N⁴LO contribution to the 3NF in terms of g_A , M_π , F_π and the renormalized LECs \bar{l}_i , \bar{d}_i , \bar{e}_i using the above relations leads to finite matrix elements provided the “rotation angles” $\alpha_{9,10,11}$ of the additional unitary transformations are chosen as:

$$\alpha_{10} = -\frac{1}{4}(1 - 2\alpha_9), \quad \alpha_{11} = \frac{1}{4}(1 - 2\alpha_9). \quad (3.15)$$

Notice that while the parameter α_9 is unfixed, the resulting 3NF turns out to be α_9 -independent. This leads to an unambiguous result for the 3NF at this order. We further emphasize that the obtained relations for $\alpha_{10,11}$ also constrain the form of the remaining N⁴LO 3NF contributions, the four-nucleon force and the subleading-loop expressions for the exchange current operators.

The final, renormalized N⁴LO contributions to the functions \mathcal{A} and \mathcal{B} in Eq. (3.3) have the form:

$$\begin{aligned} \mathcal{A}^{(5)}(q_2) &= \frac{g_A}{4608\pi^2 F_\pi^6} \left[M_\pi^2 q_2^2 (F_\pi^2 (2304\pi^2 g_A (4\bar{e}_{14} + 2\bar{e}_{19} - \bar{e}_{22} - \bar{e}_{36}) - 2304\pi^2 \bar{d}_{18} c_3) \right. \\ &\quad \left. + g_A (144c_1 - 53c_2 - 90c_3)) + M_\pi^4 (F_\pi^2 (4608\pi^2 \bar{d}_{18} (2c_1 - c_3) + 4608\pi^2 g_A (2\bar{e}_{14} + 2\bar{e}_{19} - \bar{e}_{36} - 4\bar{e}_{38})) \right. \end{aligned}$$

¹ To simplify the notation, we use here dimensionful ϵ_i in contrast to that reference.

$$\begin{aligned}
& + g_A (72 (64\pi^2 \bar{l}_3 + 1) c_1 - 24c_2 - 36c_3) + q_2^4 (2304\pi^2 \bar{e}_{14} F_\pi^2 g_A - 2g_A(5c_2 + 18c_3)) \Big] \\
& - \frac{g_A^2}{768\pi^2 F_\pi^6} L(q_2) (M_\pi^2 + 2q_2^2) (4M_\pi^2(6c_1 - c_2 - 3c_3) + q_2^2(-c_2 - 6c_3)) , \\
\mathcal{B}^{(5)}(q_2) = & - \frac{g_A}{2304\pi^2 F_\pi^6} \left[M_\pi^2 (F_\pi^2 (1152\pi^2 \bar{d}_{18} c_4 - 1152\pi^2 g_A(2\bar{e}_{17} + 2\bar{e}_{21} - \bar{e}_{37})) + 108g_A^3 c_4 + 24g_A c_4) \right. \\
& \left. + q_2^2 (5g_A c_4 - 1152\pi^2 \bar{e}_{17} F_\pi^2 g_A) \right] + \frac{g_A^2 c_4}{384\pi^2 F_\pi^6} L(q_2) (4M_\pi^2 + q_2^2) , \tag{3.16}
\end{aligned}$$

where the loop function $L(q)$ is defined according to

$$L(q) = \frac{\sqrt{q^2 + 4M_\pi^2}}{q} \log \frac{\sqrt{q^2 + 4M_\pi^2} + q}{2M_\pi} . \tag{3.17}$$

Interestingly, we observe that there are no $1/m$ -contributions to the two-pion exchange 3NF at this order. In particular, no $N^4\text{LO}$ contributions emerge from diagrams (18) and (19) in Fig. 2 since all leading (subleading) $1/m$ -corrections to the πNN ($\pi\pi NN$) vertex involve at least one time derivative. When evaluating the corresponding Feynman diagrams, these time derivatives generate insertions of the nucleon kinetic energy which are further suppressed by the factor Q/m . In addition, diagrams (20) and (21) are found not to generate any irreducible pieces.

The expressions for the 2π -exchange 3NF up to $N^4\text{LO}$ discussed above depend on a number of low-energy constants. Here and in what follows, we use the values²

$$g_A = 1.267 , \quad F_\pi = 92.4 \text{ MeV} , \quad M_\pi = 138.03 \text{ MeV} . \tag{3.18}$$

The LECs c_i , \bar{d}_i and \bar{e}_i can be most naturally determined from pion-nucleon scattering (at least) at the subleading-loop order (i.e. Q^4). The heavy-baryon analyses of pion-nucleon scattering at orders Q^3 and Q^4 can be found in Refs. [32, 45, 46], see also Refs. [44, 47, 48] for the calculations within the manifestly covariant framework, Ref. [49] for a related calculation which extends chiral EFT to higher energies by employing constraints set by causality and unitarity and Ref. [50] for a recent review on baryon chiral perturbation theory. Unfortunately, we cannot use the values of the LECs obtained in these studies since we use a different counting scheme for the nucleon mass in the few-nucleon sector, namely $Q/m \sim Q^2/\Lambda_\chi^2$ [51] rather than $m \sim \Lambda_\chi$ as used in the single-nucleon sector, see [52] for an extended discussion. In the next section, we re-analyze pion-nucleon scattering at order Q^4 in the heavy-baryon approach utilizing our counting scheme for the nucleon mass and determine all relevant LECs from a fit to the available partial wave analyses.

IV. DETERMINATION OF THE LECs FROM πN SCATTERING AT ORDER Q^4

In the center-of-mass system (cms), the amplitude for the reaction $\pi^a(q_1) + N(p_1) \rightarrow \pi^b(q_2) + N(p_2)$ with $p_{1,2}$ and $q_{1,2}$ being the corresponding four-momenta and a, b referring to the pion isospin quantum numbers, takes the form:

$$T_{\pi N}^{ba} = \frac{E + m}{2m} \left(\delta^{ba} \left[g^+(\omega, t) + i\vec{\sigma} \cdot \vec{q}_2 \times \vec{q}_1 h^+(\omega, t) \right] + i\epsilon^{bac} \tau^c \left[g^-(\omega, t) + i\vec{\sigma} \cdot \vec{q}_2 \times \vec{q}_1 h^-(\omega, t) \right] \right) . \tag{4.19}$$

Here, $\omega = q_1^0 = q_2^0$ is the pion cms energy, $E_1 = E_2 \equiv E = (\vec{q}^2 + m^2)^{1/2}$ the nucleon energy and $\vec{q}_1^2 = \vec{q}_2^2 \equiv \vec{q}^2 = ((s - M_\pi^2 - m^2)^2 - 4m^2 M_\pi^2)/(4s)$. Further, $t = (q_1 - q_2)^2$ is the invariant momentum transfer squared while s denotes the total cms energy squared. The quantities $g^\pm(\omega, t)$ ($h^\pm(\omega, t)$) refer to the isoscalar and isovector non-spin-flip (spin-flip) amplitudes and can be calculated in chiral perturbation theory. In Appendix B, we show the contributions to the amplitudes up to and including the order Q^4 using the same counting scheme for the nucleon mass as in the

² Since we employ exact isospin limit in this work, we do not distinguish between the charge and neutral pion masses and use $M_\pi = 2M_{\pi^+}/3 + M_{\pi^0}/3$.

derivation of the nuclear forces. It is important to emphasize that terms in Eq. (B.4) proportional to the LECs \bar{e}_{19} , \bar{e}_{20} , \bar{e}_{21} , \bar{e}_{22} , \bar{e}_{35} , \bar{e}_{36} , \bar{e}_{37} , \bar{e}_{38} and \bar{l}_3 can be generated from the Q^2 -terms by shifting the LECs c_i as follows [45]:

$$\begin{aligned} c_1 &\rightarrow c_1 - 2M_\pi^2 \left(\bar{e}_{22} - 4\bar{e}_{38} - \frac{\bar{l}_3 c_1}{F_\pi^2} \right), \\ c_2 &\rightarrow c_2 + 8M_\pi^2 (\bar{e}_{20} + \bar{e}_{35}), \\ c_3 &\rightarrow c_3 + 4M_\pi^2 \left(2\bar{e}_{19} - \bar{e}_{22} - \bar{e}_{36} + 2\frac{\bar{l}_3 c_1}{F_\pi^2} \right), \\ c_4 &\rightarrow c_4 + 4M_\pi^2 (2\bar{e}_{21} - \bar{e}_{37}). \end{aligned} \quad (4.20)$$

This implies that one cannot extract these combinations of \bar{e}_i and c_i separately from the πN scattering data. We, therefore, follow Ref. [45] and absorb these linear combinations into redefinition of the c_i 's by setting

$$\bar{e}_{22} - 4\bar{e}_{38} - \frac{\bar{l}_3 c_1}{F_\pi^2} = 0, \quad \bar{e}_{20} + \bar{e}_{35} = 0, \quad 2\bar{e}_{19} - \bar{e}_{22} - \bar{e}_{36} + 2\frac{\bar{l}_3 c_1}{F_\pi^2} = 0, \quad 2\bar{e}_{21} - \bar{e}_{37} = 0, \quad (4.21)$$

without loss of generality. Choosing another prescription would result in corrections generated by the loops involving c_i that are beyond the order we are working. Notice further that with the above convention, there is no dependence anymore on the LEC \bar{l}_3 . The LEC \bar{d}_{18} can be fixed by means of the Goldberger-Treiman discrepancy

$$g_{\pi NN} = \frac{g_A m}{F_\pi} \left(1 - \frac{2M_\pi^2 \bar{d}_{18}}{g_A} \right), \quad (4.22)$$

where for $g_{\pi NN}$ we adopt the value from Ref. [53]: $g_{\pi NN}^2/(4\pi) \simeq 13.54$ which also agrees with the recent determination in Ref. [54] based on the Goldberger-Miyazawa-Oehme sum rule and utilizing the most accurate available data on the pion-nucleon scattering lengths. Again, at the order we are working, we are free to set $\bar{d}_{18} = 0$ provided we use the effective value for g_A ,

$$g_A = \frac{F_\pi g_{\pi NN}}{m} \simeq 1.285, \quad (4.23)$$

in all expressions. We adopt this convention in the following analysis. Thus, we are finally left with 13 independent (linear combinations of the) low energy constants to be fixed from a fit to the data, namely $c_{1,2,3,4}$, $\bar{d}_1 + \bar{d}_2$, \bar{d}_3 , \bar{d}_5 , $\bar{d}_{14} - \bar{d}_{15}$ and $\bar{e}_{14,15,16,17,18}$.

The fit can be most conveniently performed in the partial wave basis using the available partial wave analyses. In order to estimate a possible uncertainty of the extracted parameters, we considered two different partial wave analyses in our fitting procedure, namely the one of Ref. [56] by the group at the George Washington University, to be referred as GW, and the Karlsruhe-Helsinki analysis of Ref. [57]), to be referred as KH. The energy range of the data fitted corresponds to the πN laboratory momenta $p_{\text{Lab}} < 150$ MeV/c. At higher energies the convergence of the chiral expansion becomes doubtful. We follow the strategy which is similar to the one utilized in Ref. [32] and assign the same relative error to all empirical data points.

The partial wave amplitudes $f_{l\pm}^\pm(s)$, where l refers to the orbital angular momentum and the subscript ' \pm ' to the total angular momentum ($j = l \pm s$), are given in terms of the invariant amplitudes via

$$f_{l\pm}^\pm(s) = \frac{E+m}{16\pi\sqrt{s}} \int_{-1}^{+1} dz \left[g^\pm P_l(z) + \vec{q}^2 h^\pm (P_{l\pm 1}(z) - zP_l(z)) \right],$$

where $z = \cos(\theta)$ is the angular variable ($t = 2\vec{q}^2(z-1)$). The amplitude in the isospin basis are related to $f_{l\pm}^\pm$ as follows

$$f_{l\pm}^{1/2} = f_{l\pm}^+ + 2f_{l\pm}^-, \quad f_{l\pm}^{3/2} = f_{l\pm}^+ - f_{l\pm}^-.$$

The phase shift for a partial wave amplitude with isospin I is obtained using the following unitarization prescription³ [32]:

$$\delta_{l\pm}^I(s) = \arctan \left(|\vec{q}| \Re f_{l\pm}^I(s) \right), \quad (4.24)$$

³ It should be understood that this unitarization prescription goes, strictly speaking, beyond the chiral power counting. The resulting model dependence is, however, very small due to the smallness of the phase shifts with the only exception of the P_{33} partial wave, see [55] for a related discussion.

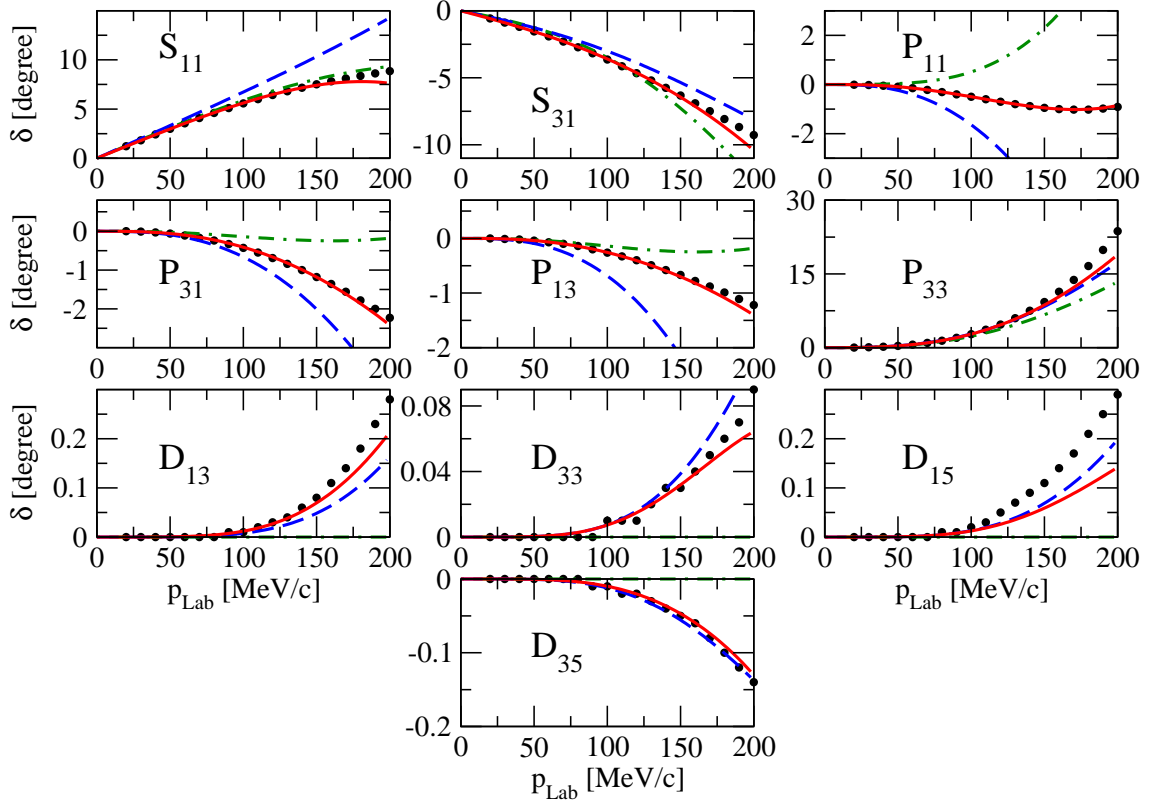


FIG. 3: Results of the fit for πN s , p and d -wave phase shifts using the GW partial wave analysis of Ref. [56]. The solid curves correspond to the full Q^4 results, the dashed curves to the order- Q^3 results, and the dashed-dotted curves to the order- Q^2 calculation.

which reflects the absence of inelasticity below the two-pion production threshold.

We performed a combined fit for all s -, p -, and d -waves since d -waves are the highest partial waves where the order- Q^4 counter terms contribute. The results of the fits using the GW and KH partial wave analyses are visualized in Figs. 3 and 4, respectively. In these figures we show the full, order- Q^4 results (solid curves) as well as the phase shifts calculated up to the order Q^3 (dashed curves) and Q^2 (dashed-dotted curves) using the same parameters (from the order- Q^4 fit) in all curves. In the fitted region (from threshold up to $p_{\text{Lab}} = 150$ MeV/c), a good description of the data is achieved. As one would expect the convergence pattern when going from Q^2 to Q^4 is getting worse with increasing the pion momenta. Interestingly, the d -waves are rather well reproduced already at the order Q^3 where there are no counter terms or other contributions depending on free parameters. Both the tree-level and finite loop contributions are important for those four partial waves. Our results for the phase shifts are similar and of a similar quality as the ones reported in Ref. [45].

We finally turn to the discussion of the extracted parameters. The obtained values of the low energy constants are collected in Table I. As one can see from the table, the LECs c_i and \bar{d}_i turn out to come out rather similar for the two partial wave analyses. The difference does not exceed 30% except for the LECs c_1 and \bar{d}_5 which are, however, considerably smaller than the other c_i 's and \bar{d}_i 's, respectively. The same conclusion about stability can be drawn for the LECs \bar{e}_{14} and \bar{e}_{17} . These are the only counter terms contributing to d -waves, which is why these two constants are strongly constrained by the threshold behavior of the d -wave phase shifts. In contrast, the other \bar{e}_i 's are very sensitive to the energy dependence of the s - and p -wave amplitudes and, therefore, vary strongly from one analysis to another. Notice, however, that all extracted constants are of a natural size except for the combination $\bar{d}_{14} - \bar{d}_{15}$ and \bar{e}_{15} which appear to be somewhat large.

We stress that one cannot directly compare the LECs \bar{d}_i and \bar{e}_i from our fits to the ones obtained in Refs. [32],[45]

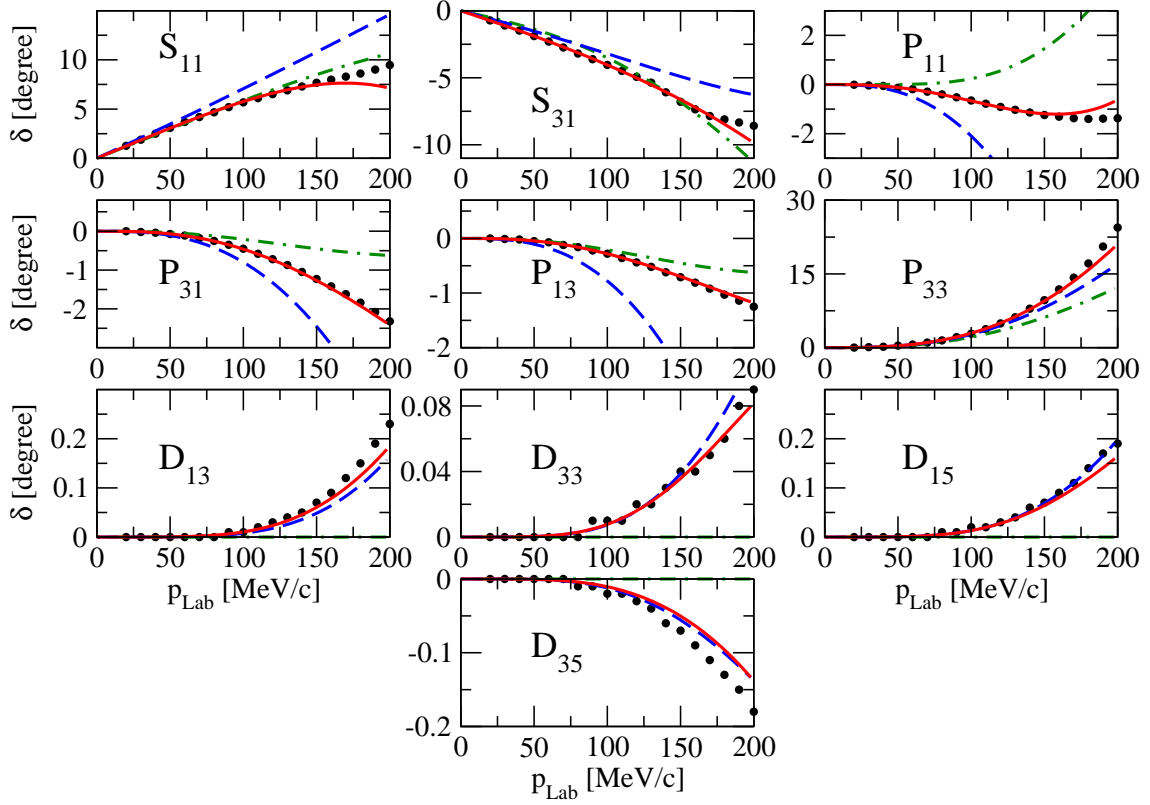


FIG. 4: Results of the fit for πN s , p and d -wave phase shifts using the KH partial wave analysis of Ref. [57]. The solid curves correspond to the full Q^4 results, the dashed curves to the order- Q^3 results, and the dashed-dotted curves to the order- Q^2 calculation.

using heavy-baryon chiral perturbation theory at orders Q^3 and Q^4 , respectively, because of a different power counting schemes in the two approaches. On the other hand, it is comforting to see that the extracted values for the c_i -, \bar{d}_i - and even some of the \bar{e}_i -coefficients are comparable to the ones found in Ref. [45] in the fit with the LECs c_i being set to their order- Q^3 values, see table 4 of that work. We also stress that the values for $c_{1,3,4}$ obtained from the fit to the KH partial wave analysis are in an excellent agreement with the ones determined at order Q^3 by using chiral perturbation theory inside the Mandelstam triangle [58]. It is also worth mentioning that the values of $c_{3,4}$ are in a good agreement with the ones determined from the new partial wave analysis of proton-proton and neutron-proton scattering data of Ref. [59].

It should be emphasized that one can obtain a considerably better description of the πN phase shifts at orders Q^2 and Q^3 by allowing for the LECs c_i and \bar{d}_i to be tuned rather than keeping their values fixed at order Q^4 . In fact, the values of c_i are well known to change significantly when performing fits at orders Q^2 and Q^3 . Using the KH partial wave analysis, employing the order- Q^2 expressions for the amplitudes and utilizing the same fitting procedure

	c_1	c_2	c_3	c_4	$\bar{d}_1 + \bar{d}_2$	\bar{d}_3	\bar{d}_5	$\bar{d}_{14} - \bar{d}_{15}$	\bar{e}_{14}	\bar{e}_{15}	\bar{e}_{16}	\bar{e}_{17}	\bar{e}_{18}
fit to GW, Ref. [56]	-1.13	3.69	-5.51	3.71	5.57	-5.35	0.02	-10.26	1.75	-5.80	1.76	-0.58	0.96
fit to KH, Ref. [57]	-0.75	3.49	-4.77	3.34	6.21	-6.83	0.78	-12.02	1.52	-10.41	6.08	-0.37	3.26

TABLE I: Low-energy constants obtained from a fit to the empirical s , p - and d -wave pion-nucleon phase shifts using partial wave analysis of Ref. [56] and of Ref. [57]. Values of the LECs are given in GeV^{-1} , GeV^{-2} and GeV^{-3} for the c_i , \bar{d}_i and \bar{e}_i , respectively.

as before, we end up with the following values for the c_i 's:

$$c_1^{\text{KH}} = -0.26 \text{ GeV}^{-1}, \quad c_2^{\text{KH}} = 2.02 \text{ GeV}^{-1}, \quad c_3^{\text{KH}} = -2.80 \text{ GeV}^{-1}, \quad c_4^{\text{KH}} = 2.01 \text{ GeV}^{-1}, \quad (4.25)$$

while the GW partial wave analysis yields:

$$c_1^{\text{GW}} = -0.58 \text{ GeV}^{-1}, \quad c_2^{\text{GW}} = 2.02 \text{ GeV}^{-1}, \quad c_3^{\text{GW}} = -3.14 \text{ GeV}^{-1}, \quad c_4^{\text{GW}} = 2.19 \text{ GeV}^{-1}. \quad (4.26)$$

Notice that $c_{2,3,4}$ turn out to be somewhat smaller in magnitude than the ones extracted from the order- Q^2 fit to the s - and p -wave πN threshold coefficients [20].⁴ We will come back to the issue of optimizing the description of the data at lower orders of the chiral expansion in the next section. Notice, however, that in spite of such a possibility, we believe that the results shown in Figs. 3 and 4 provide a more realistic picture of the convergence of the heavy-baryon chiral perturbation theory for pion-nucleon scattering.

V. RESULTS FOR THE TWO-PION EXCHANGE 3NF

With all relevant LECs being determined from pion-nucleon scattering, we are now in the position to analyze the convergence of the chiral expansion for the two-pion exchange 3NF. In Fig. 5, we show the results for the functions $\mathcal{A}(q_2)$ and $\mathcal{B}(q_2)$ for small values of the momentum transfer q_2 , $q_2 < 300$ MeV at various orders in the chiral expansion. More precisely, we plot $\mathcal{A}^{(3)}$, $\mathcal{A}^{(3)} + \mathcal{A}^{(4)}$ and $\mathcal{A}^{(3)} + \mathcal{A}^{(4)} + \mathcal{A}^{(5)}$ as well as $\mathcal{B}^{(3)}$, $\mathcal{B}^{(3)} + \mathcal{B}^{(4)}$ and $\mathcal{B}^{(3)} + \mathcal{B}^{(4)} + \mathcal{B}^{(5)}$ using the values of the LECs c_i , \bar{d}_i and \bar{e}_i determined from the order- Q^4 fit to the KH and GW partial wave analyses as described in the previous section. We use here the same, fixed values for the LECs c_i (and \bar{d}_i) listed in Table I at all orders and adopt the same conventions regarding the LECs as in the case of pion-nucleon scattering, see Eqs. (4.21) and (4.23). Notice that $\mathcal{A}^{(5)}$ and $\mathcal{B}^{(5)}$ do not depend on the LECs $\bar{e}_{15,16,18}$ which are very sensitive to a particular choice of the partial wave analysis in pion-nucleon scattering, see Table I. The relevant LECs $\bar{e}_{14,17}$ are, on the contrary, rather stable as they are well determined in πN d -waves.

One observes a very good convergence for the function \mathcal{A} with the subleading-order result (i.e. N^3LO) being very close to the one at N^4LO . It is also comforting to see that both partial wave analyses lead to similar results for this quantity. The dependence on the input for pion-nucleon phase shifts for \mathcal{A} is bigger than the shift from N^3LO to N^4LO which can serve as a (conservative) estimation of the theoretical uncertainty at N^4LO . The convergence for the function \mathcal{B} is somewhat slower with the shift from N^3LO to N^4LO being of the order of $\sim 30\%$. Also the difference between the two partial wave analyses of the order of $\sim 20\%$ is larger than for the function \mathcal{A} . It should be understood that an accurate description of the low-energy pion-nucleon scattering data at different orders does not automatically guarantee a good convergence of the chiral expansion for \mathcal{A} and \mathcal{B} . In particular, these quantities do not depend on the LECs \bar{d}_i (to the order considered) which contribute to πN phase shifts. Thus, the observed reasonable convergence for the 2π -exchange 3NF is a highly non-trivial test of the theoretical approach.

Given that the q_2 -dependence of \mathcal{A} , \mathcal{B} does not change significantly when going from N^2LO to N^4LO , it is clear that the final result at N^4LO can be well approximated by the N^2LO expressions with the appropriately tuned LECs $c_{1,3,4}$. This feature is visualized in Fig. 6, where the dotted lines show $\mathcal{A}^{(3)}(q_2)$ and $\mathcal{B}^{(3)}(q_2)$ from Eq. (3.5) with

$$c_1^{\text{KH}} = -0.37 \text{ GeV}^{-1}, \quad c_3^{\text{KH}} = -2.71 \text{ GeV}^{-1}, \quad c_4^{\text{KH}} = 1.41 \text{ GeV}^{-1}. \quad (5.27)$$

These values of c_i 's are adjusted in such a way that $\mathcal{A}^{(3)}(0)$, $\mathcal{B}^{(3)}(0)$ and the curvature of the function $\mathcal{A}^{(3)}(q_2)$ at $q_2 = 0$ coincide with the ones resulting from $\mathcal{A}^{(3)} + \mathcal{A}^{(4)} + \mathcal{A}^{(5)}$, $\mathcal{B}^{(3)} + \mathcal{B}^{(4)} + \mathcal{B}^{(5)}$ and using the LECs from the KH fits to the πN data. Not surprisingly, the c_i 's in Eq. (5.27) are fairly close to the Q^2 -fit values in Eq. (4.25). We also show in Fig. 6 the functions $\mathcal{A}^{(3)}(q_2)$, $\mathcal{B}^{(3)}(q_2)$ with the c_i 's from Eq. (4.25) (dashed-dotted lines). When using the GW partial wave analysis, the resulting values of the c_i 's slightly change to:

$$c_1^{\text{GW}} = -0.73 \text{ GeV}^{-1}, \quad c_3^{\text{GW}} = -3.38 \text{ GeV}^{-1}, \quad c_4^{\text{GW}} = 1.69 \text{ GeV}^{-1}. \quad (5.28)$$

The values in Eqs. (5.27) and (5.28) can be regarded as the recommended ones when the 3NF is taken into account at N^2LO . One should, however, always keep in mind that the true theoretical uncertainty for the 2π -exchange 3NF at N^2LO is sizable, see Fig. 5.

⁴ This indicates that the order- Q^2 representation of the amplitudes does not provide the appropriate description of the data in the whole momentum range used in our fits.

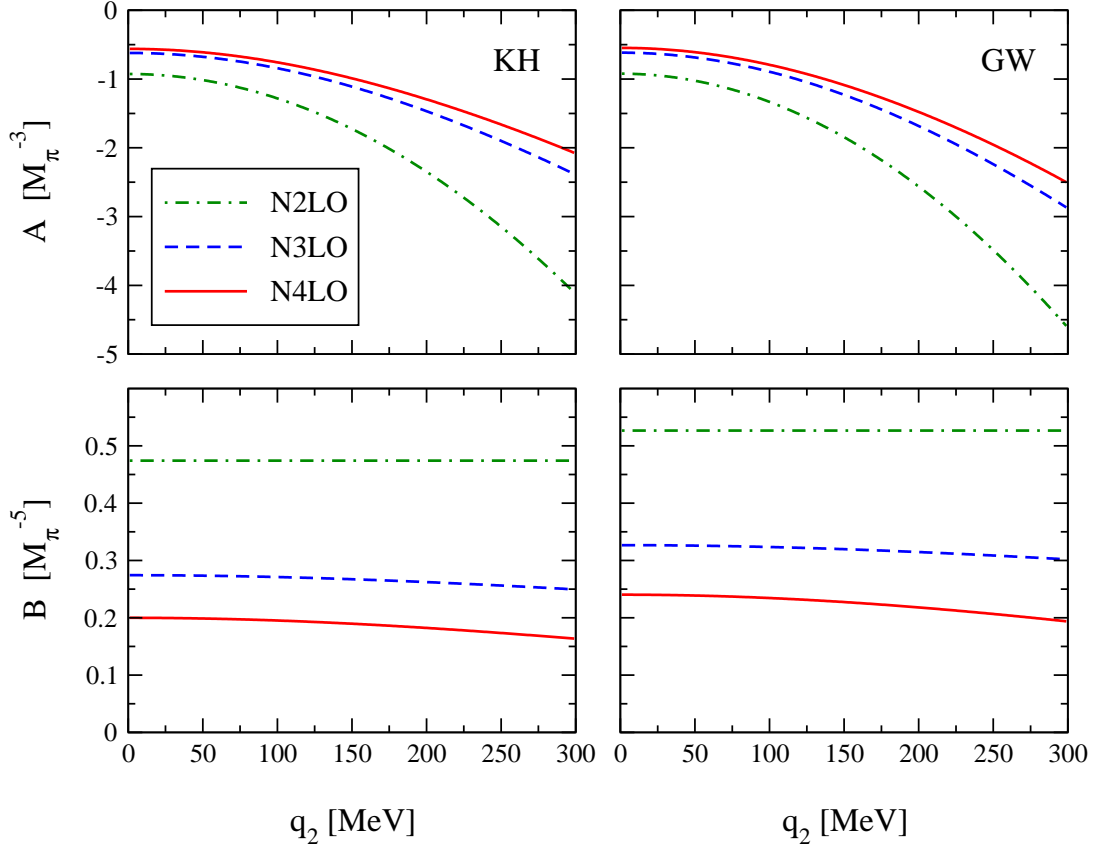


FIG. 5: Chiral expansion of the functions $\mathcal{A}(q_2)$ and $\mathcal{B}(q_2)$ entering the two-pion exchange 3NF in Eq. (3.3) up to N⁴LO. Left (right) panel shows the results obtained with the LECs determined from the order- Q^4 fit to the pion-nucleon partial wave analysis of Ref. [57] (Ref. [56]) and listed in Table I. Dashed, dashed-dotted and solid lines correspond to $\mathcal{A}^{(3)}$, $\mathcal{A}^{(3)} + \mathcal{A}^{(4)}$ and $\mathcal{A}^{(3)} + \mathcal{A}^{(4)} + \mathcal{A}^{(5)}$ in the upper plots while $\mathcal{B}^{(3)}$, $\mathcal{B}^{(3)} + \mathcal{B}^{(4)}$ and $\mathcal{B}^{(3)} + \mathcal{B}^{(4)} + \mathcal{B}^{(5)}$ in the lower plots.

VI. SUMMARY AND CONCLUSIONS

In this paper, we have analyzed the longest-range contribution to the three-nucleon force at N⁴LO utilizing the heavy-baryon formulation of chiral EFT with pions and nucleons as the only explicit degrees of freedom. For this particular topology, the N⁴LO corrections already provide the sub-subleading contribution, so that one can address the question of convergence of the chiral expansion. The pertinent results of our study can be summarized as follows.

- We worked out the N⁴LO contributions to the 2π -exchange 3NF. The unitary ambiguity of the Hamilton operator can be parametrized at this order by three additional unitary transformations. We found that two of the corresponding “rotation angles”, namely α_{10} and α_{11} , are fixed in terms of the remaining one α_9 if one requires that the resulting 3NF matrix elements are finite (renormalizability constraint). The parameter α_9 does not enter the expressions for the 3NF at N⁴LO. These findings will impact the results for the remaining 3NF contributions which are not considered in this paper.
- In order to determine the low-energy constants c_i , \bar{d}_i and \bar{e}_i contributing to the 2π -exchange 3NF, we re-analyzed pion-nucleon scattering at order Q^4 employing exactly the same power counting scheme as in the derivation of the nuclear forces. We used the available partial wave analyses of the pion-nucleon scattering data to determine all relevant LECs. The resulting values turn out to be rather stable and agree well with the determinations by other groups.
- With all LECs being fixed from pion-nucleon scattering as discussed above, we found a good/reasonable con-

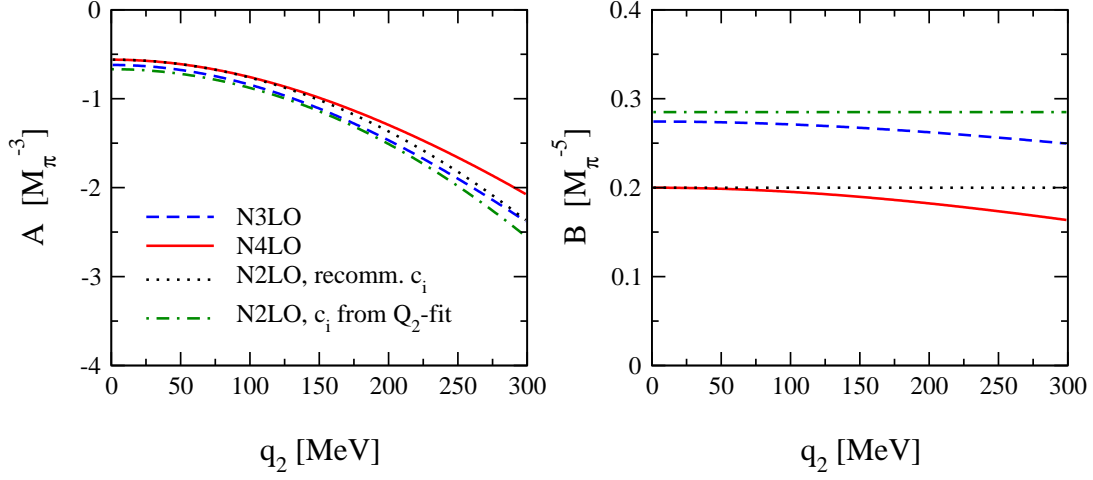


FIG. 6: Chiral expansion of the functions $\mathcal{A}(q_2)$ and $\mathcal{B}(q_2)$ using the LECs determined from the fits to the KH πN partial wave analysis. The dashed and solid lines are the same as in Fig. 5. The dotted and dashed-dotted lines show $\mathcal{A}^{(3)}(q_2)$, $\mathcal{B}^{(3)}(q_2)$ with the LECs c_i taken from Eq. (5.27) and (4.25), respectively.

vergence of the chiral expansion for the functions \mathcal{A} and \mathcal{B} which parametrize the (static part of the) two-pion exchange 3NF. We also provide the recommended values of the LECs $c_{1,3,4}$ which allow one to approximate the full, N⁴LO result for the 2π -exchange 3NF by the N²LO expressions.

As explained in the introduction, one generally expects important contributions to the nuclear forces associated with the intermediate Δ -excitations. The observed (reasonable) convergence pattern for the longest-range 3NF is not surprising given that effects of the Δ -isobar are, to a large extent, accounted for already in the leading contribution to this topology (i.e. at N²LO) through resonance saturation of the LECs $c_{3,4}$. The situation is different for the two-pion-one-pion exchange and ring 3NF topologies, whose leading contributions at N³LO are completely missing effects of the Δ -isobar. The corresponding N⁴LO corrections are, therefore, expected to be large and need to be worked out. Work along these lines is in progress.

Acknowledgments

We are grateful to Ulf-G. Meißner for helpful comments on the manuscript and Achim Schwenk for useful discussions. This work is supported by the EU HadronPhysics3 project “Study of strongly interacting matter”, by the European Research Council (ERC-2010-StG 259218 NuclearEFT) and by the DFG (TR 16, “Subnuclear Structure of Matter”).

Appendix A: Formal algebraic structure of the N⁴LO corrections

In this Appendix we list the formal operator structure of the various N⁴LO contributions to the nuclear Hamiltonian relevant for the present calculations. A detailed discussion on the method of unitary transformation including the explicit form of the unitary operator at lower orders in the chiral expansion can be found in Ref. [39].

- terms $\propto g_A^4 c_i$:

$$V = \eta \left[\alpha_9 \left(H_{21}^{(1)} \frac{\lambda^1}{E_\pi} H_{21}^{(1)} \eta H_{21}^{(1)} \frac{\lambda^1}{E_\pi} H_{21}^{(1)} \frac{\lambda^2}{E_\pi^2} H_{22}^{(3)} - H_{21}^{(1)} \frac{\lambda^1}{E_\pi} H_{21}^{(1)} \eta H_{22}^{(3)} \frac{\lambda^2}{E_\pi^2} H_{21}^{(1)} \frac{\lambda^1}{E_\pi} H_{21}^{(1)} \right) \right]$$

$$\begin{aligned}
V = & \eta \left[\alpha_9 \left(-H_{20}^{(2)} \eta H_{21}^{(1)} \frac{\lambda^1}{E_\pi} H_{21}^{(1)} \frac{\lambda^2}{E_\pi^2} H_{22}^{(3)} + H_{20}^{(2)} \eta H_{22}^{(3)} \frac{\lambda^2}{E_\pi^2} H_{21}^{(1)} \frac{\lambda^1}{E_\pi} H_{21}^{(1)} + H_{21}^{(1)} \frac{\lambda^1}{E_\pi} H_{21}^{(1)} \frac{\lambda^2}{E_\pi^2} H_{22}^{(3)} \eta H_{20}^{(2)} \right. \right. \\
& \left. \left. - H_{22}^{(3)} \frac{\lambda^2}{E_\pi^2} H_{21}^{(1)} \frac{\lambda^1}{E_\pi} H_{21}^{(1)} \eta H_{20}^{(2)} \right) + \alpha_{10} \left(-H_{20}^{(2)} \eta H_{21}^{(1)} \frac{\lambda^1}{E_\pi^2} H_{21}^{(1)} \frac{\lambda^2}{E_\pi} H_{22}^{(3)} + H_{20}^{(2)} \eta H_{22}^{(3)} \frac{\lambda^2}{E_\pi} H_{21}^{(1)} \frac{\lambda^1}{E_\pi^2} H_{21}^{(1)} \right. \right. \\
& \left. \left. + H_{21}^{(1)} \frac{\lambda^1}{E_\pi^2} H_{21}^{(1)} \frac{\lambda^2}{E_\pi} H_{22}^{(3)} \eta H_{20}^{(2)} - H_{22}^{(3)} \frac{\lambda^2}{E_\pi} H_{21}^{(1)} \frac{\lambda^1}{E_\pi^2} H_{21}^{(1)} \eta H_{20}^{(2)} \right) + \alpha_{11} \left(-H_{20}^{(2)} \eta H_{21}^{(1)} \frac{\lambda^1}{E_\pi} H_{22}^{(3)} \frac{\lambda^1}{E_\pi^2} H_{21}^{(1)} \right. \right. \\
& \left. \left. + H_{20}^{(2)} \eta H_{21}^{(1)} \frac{\lambda^1}{E_\pi^2} H_{22}^{(3)} \frac{\lambda^1}{E_\pi} H_{21}^{(1)} + H_{21}^{(1)} \frac{\lambda^1}{E_\pi} H_{22}^{(3)} \frac{\lambda^1}{E_\pi^2} H_{21}^{(1)} \eta H_{20}^{(2)} - H_{21}^{(1)} \frac{\lambda^1}{E_\pi^2} H_{22}^{(3)} \frac{\lambda^1}{E_\pi} H_{21}^{(1)} \eta H_{20}^{(2)} \right) \right]
\end{aligned}$$

$$\begin{aligned}
& + \frac{1}{2} \left(H_{20}^{(2)} \eta H_{21}^{(1)} \frac{\lambda^1}{E_\pi} H_{21}^{(1)} \frac{\lambda^2}{E_\pi^2} H_{22}^{(3)} + H_{20}^{(2)} \eta H_{21}^{(1)} \frac{\lambda^1}{E_\pi} H_{22}^{(3)} \frac{\lambda^1}{E_\pi^2} H_{21}^{(1)} + H_{20}^{(2)} \eta H_{21}^{(1)} \frac{\lambda^1}{E_\pi^2} H_{21}^{(1)} \frac{\lambda^2}{E_\pi} H_{22}^{(3)} \right. \\
& + H_{20}^{(2)} \eta H_{21}^{(1)} \frac{\lambda^1}{E_\pi^2} H_{22}^{(3)} \frac{\lambda^1}{E_\pi} H_{21}^{(1)} + H_{20}^{(2)} \eta H_{22}^{(3)} \frac{\lambda^2}{E_\pi} H_{21}^{(1)} \frac{\lambda^1}{E_\pi^2} H_{21}^{(1)} + H_{20}^{(2)} \eta H_{22}^{(3)} \frac{\lambda^2}{E_\pi^2} H_{21}^{(1)} \frac{\lambda^1}{E_\pi} H_{21}^{(1)} \\
& - 2H_{21}^{(1)} \frac{\lambda^1}{E_\pi} H_{20}^{(2)} \frac{\lambda^1}{E_\pi} H_{21}^{(1)} \frac{\lambda^2}{E_\pi} H_{22}^{(3)} - 2H_{21}^{(1)} \frac{\lambda^1}{E_\pi} H_{20}^{(2)} \frac{\lambda^1}{E_\pi} H_{22}^{(3)} \frac{\lambda^1}{E_\pi} H_{21}^{(1)} - 2H_{21}^{(1)} \frac{\lambda^1}{E_\pi} H_{21}^{(1)} \frac{\lambda^2}{E_\pi} H_{20}^{(2)} \frac{\lambda^2}{E_\pi} H_{22}^{(3)} \\
& + H_{21}^{(1)} \frac{\lambda^1}{E_\pi} H_{21}^{(1)} \frac{\lambda^2}{E_\pi^2} H_{22}^{(3)} \eta H_{20}^{(2)} - 2H_{21}^{(1)} \frac{\lambda^1}{E_\pi} H_{22}^{(3)} \frac{\lambda^1}{E_\pi} H_{20}^{(2)} \frac{\lambda^1}{E_\pi} H_{21}^{(1)} + H_{21}^{(1)} \frac{\lambda^1}{E_\pi} H_{22}^{(3)} \frac{\lambda^1}{E_\pi^2} H_{21}^{(1)} \eta H_{20}^{(2)} \\
& + H_{21}^{(1)} \frac{\lambda^1}{E_\pi^2} H_{21}^{(1)} \frac{\lambda^2}{E_\pi} H_{22}^{(3)} \eta H_{20}^{(2)} + H_{21}^{(1)} \frac{\lambda^1}{E_\pi^2} H_{22}^{(3)} \frac{\lambda^1}{E_\pi} H_{21}^{(1)} \eta H_{20}^{(2)} - 2H_{22}^{(3)} \frac{\lambda^2}{E_\pi} H_{20}^{(2)} \frac{\lambda^2}{E_\pi} H_{21}^{(1)} \frac{\lambda^1}{E_\pi} H_{21}^{(1)} \\
& \left. - 2H_{22}^{(3)} \frac{\lambda^2}{E_\pi} H_{21}^{(1)} \frac{\lambda^1}{E_\pi} H_{20}^{(2)} \frac{\lambda^1}{E_\pi} H_{21}^{(1)} + H_{22}^{(3)} \frac{\lambda^2}{E_\pi} H_{21}^{(1)} \frac{\lambda^1}{E_\pi^2} H_{21}^{(1)} \eta H_{20}^{(2)} + H_{22}^{(3)} \frac{\lambda^2}{E_\pi^2} H_{21}^{(1)} \frac{\lambda^1}{E_\pi} H_{21}^{(1)} \eta H_{20}^{(2)} \right) \eta. \quad (\text{A.2})
\end{aligned}$$

Here and in what follows, we adopt the notation of Refs. [15, 39–41]. In particular, the subscripts a and b in $H_{ab}^{(\kappa)}$ refer to the number of the nucleon and pion fields, respectively, while the superscript κ gives the inverse mass dimension of the corresponding coupling constant⁵, see Ref. [39] for more details. The chiral order associated with a given contribution can easily be read off by adding together the dimensions κ of $H_{ab}^{(\kappa)}$. More precisely, it is given by $\sum_i \kappa_i - 2$. In the above equations, η (λ) denote projection operators onto the purely nucleonic (the remaining) part of the Fock space satisfying $\eta^2 = \eta$, $\lambda^2 = \lambda$, $\eta\lambda = \lambda\eta = 0$ and $\lambda + \eta = \mathbf{1}$. The superscript i of λ^i refers to the number of pions in the corresponding intermediate state. Further, E_π denotes the total energy of the pions in the corresponding state, $E_\pi = \sum_i \sqrt{\vec{l}_i^2 + M_\pi^2}$, with \vec{l}_i the corresponding pion momenta. Last but not least, the parameters $\alpha_{9,10,11}$ parametrize the unitary ambiguity of the resulting nuclear Hamiltonian.

Appendix B: Chiral expansion of the invariant πN amplitudes $g^\pm(\omega, t)$ and $h^\pm(\omega, t)$

In this Appendix we give the explicit expressions for the invariant amplitudes $g^\pm(\omega, t)$ and $h^\pm(\omega, t)$ which parametrize the pion-nucleon scattering matrix at first four orders in the chiral expansion. We use here the heavy-baryon approach with the nucleon mass being counted according to $Q/m \sim Q^2/\Lambda_\chi^2$. This has the consequence that relativistic corrections are shifted to higher orders as compared to the standard approach based on the assignment $m \sim \Lambda_\chi$. Apart from this difference, our results agree with the expressions given in Ref. [45] (modulo one obvious misprint in that work).

Contributions at order Q :

$$g^+ = 0, \quad g^- = \frac{g_A^2 (2M_\pi^2 - t - 2\omega^2) + 2\omega^2}{4F_\pi^2 \omega}, \quad h^+ = -\frac{g_A^2}{2F_\pi^2 \omega}, \quad h^- = 0, \quad (\text{B.1})$$

Contributions at order Q^2 :

$$g^+ = -\frac{4c_1 M_\pi^2 - 2c_2 \omega^2 - c_3 (2M_\pi^2 - t)}{F_\pi^2}, \quad g^- = 0, \quad h^+ = 0, \quad h^- = \frac{c_4}{F_\pi^2}, \quad (\text{B.2})$$

Contributions at order Q^3 :

$$g^+ = \frac{i\sqrt{\omega^2 - M_\pi^2} (g_A^4 (M_\pi^2 - \omega^2) (2M_\pi^2 - t - 2\omega^2) + 3\omega^4)}{24\pi F_\pi^4 \omega^2} - \frac{g_A^2 \tilde{K}_0(t) (2M_\pi^4 - 5M_\pi^2 t + 2t^2)}{8F_\pi^4}$$

⁵ For $1/m$ -corrections, κ_i corresponds to the inverse power of coupling constants plus twice the power of m^{-1} . In particular, $\kappa = 2$ for the nucleon kinetic energy term H_{20} .

$$\begin{aligned}
& + \frac{g_A^2 M_\pi (4g_A^2 M_\pi^2 (2M_\pi^2 - t - 2\omega^2) + 3\omega^2 (M_\pi^2 - 2t))}{96\pi F_\pi^4 \omega^2} - \frac{g_A^2 (4M_\pi^4 - 4M_\pi^2 t + t(t + 4\omega^2))}{16F_\pi^2 m \omega^2}, \\
g^- &= \frac{(\bar{d}_1 + \bar{d}_2) (4M_\pi^2 \omega - 2t\omega)}{F_\pi^2} + \frac{4\bar{d}_3 \omega^3}{F_\pi^2} + \frac{8\bar{d}_5 M_\pi^2 \omega}{F_\pi^2} + \frac{\bar{d}_{18} g_A M_\pi^2 (-2M_\pi^2 + t + 2\omega^2)}{F_\pi^2 \omega} \\
& + \frac{\tilde{J}_0(\omega) (g_A^4 (M_\pi^2 - \omega^2) (2M_\pi^2 - t - 2\omega^2) + 6\omega^4)}{12F_\pi^4 \omega^2} + \frac{i\sqrt{\omega^2 - M_\pi^2} (g_A^4 (M_\pi^2 - \omega^2) (2M_\pi^2 - t - 2\omega^2) + 6\omega^4)}{96\pi F_\pi^4 \omega^2} \\
& + \frac{g_A^4 (3M_\pi^2 - 2\omega^2) (2M_\pi^2 - t - 2\omega^2) - g_A^2 \omega^2 (12M_\pi^2 + t) + \omega^2 (t - 6M_\pi^2)}{288\pi^2 F_\pi^4 \omega} \\
& + \frac{\tilde{I}_{20}(t) \omega (-4(2g_A^2 + 1) M_\pi^2 + 5g_A^2 t + t)}{12F_\pi^4} - \frac{(-4M_\pi^2 + t + 4\omega^2) (g_A^2 (2M_\pi^2 - t + 2\omega^2) - 2\omega^2)}{16F_\pi^2 m \omega^2}, \\
h^+ &= \frac{2(\bar{d}_{14} - \bar{d}_{15}) \omega}{F_\pi^2} + \frac{2\bar{d}_{18} g_A M_\pi^2}{F_\pi^2 \omega} + \frac{g_A^4 \tilde{J}_0(\omega) (\omega^2 - M_\pi^2)}{6F_\pi^4 \omega^2} + \frac{ig_A^4 (\omega^2 - M_\pi^2)^{3/2}}{48\pi F_\pi^4 \omega^2} - \frac{g_A^4 (3M_\pi^2 + 4\omega^2)}{144\pi^2 F_\pi^4 \omega} + \frac{g_A^2 (t - 4M_\pi^2)}{8F_\pi^2 m \omega^2}, \\
h^- &= \frac{ig_A^4 (\omega^2 - M_\pi^2)^{3/2}}{24\pi F_\pi^4 \omega^2} + \frac{g_A^2 \tilde{K}_0(t) (4M_\pi^2 - t)}{8F_\pi^4} - \frac{4g_A^4 M_\pi^3 + 3g_A^2 M_\pi \omega^2}{96\pi F_\pi^4 \omega^2} + \frac{g_A^2 (2M_\pi^2 - t - 2\omega^2) + 2\omega^2}{8F_\pi^2 m \omega^2}, \tag{B.3}
\end{aligned}$$

Contributions at order Q^4 :

$$\begin{aligned}
g^+ &= \frac{2c_1 \tilde{I}_{20}(t) M_\pi^2 (M_\pi^2 - 2t)}{F_\pi^4} + c_2 \left(-\frac{\tilde{I}_{20}(t) (4M_\pi^4 - 9M_\pi^2 t + 2t^2)}{12F_\pi^4} - \frac{6M_\pi^4 - 13M_\pi^2 t + 2t^2}{288\pi^2 F_\pi^4} + \frac{\omega (-4M_\pi^2 + t + 4\omega^2)}{F_\pi^2 m} \right) \\
& - \frac{c_3 \tilde{I}_{20}(t) (2M_\pi^4 - 5M_\pi^2 t + 2t^2)}{2F_\pi^4} + \frac{4\bar{e}_{14} (t - 2M_\pi^2)^2}{F_\pi^2} + \frac{8\bar{e}_{15} \omega^2 (2M_\pi^2 - t)}{F_\pi^2} + \frac{16\bar{e}_{16} \omega^4}{F_\pi^2} \\
& + \frac{4M_\pi^2 (2\bar{e}_{19} - \bar{e}_{22} - \bar{e}_{36} + 2\bar{l}_3 c_1 F_\pi^{-2}) (2M_\pi^2 - t)}{F_\pi^2} + \frac{16(\bar{e}_{20} + \bar{e}_{35}) M_\pi^2 \omega^2}{F_\pi^2} + \frac{8(\bar{e}_{22} - 4\bar{e}_{38} - \bar{l}_3 c_1 F_\pi^{-2}) M_\pi^4}{F_\pi^2}, \\
g^- &= -\frac{ic_1 M_\pi^2 \omega \sqrt{\omega^2 - M_\pi^2}}{\pi F_\pi^4} + \frac{ic_2 \omega^3 \sqrt{\omega^2 - M_\pi^2}}{2\pi F_\pi^4} \\
& + c_3 \left(\frac{g_A^2 M_\pi^3 (2M_\pi^2 - t - 2\omega^2)}{12\pi F_\pi^4 \omega} + \frac{i\sqrt{\omega^2 - M_\pi^2} (g_A^2 (M_\pi^2 - \omega^2) (2M_\pi^2 - t - 2\omega^2) + 6\omega^4)}{12\pi F_\pi^4 \omega} \right) \\
& + c_4 \left(-\frac{ig_A^2 (\omega^2 - M_\pi^2)^{3/2} (-2M_\pi^2 + t + 2\omega^2)}{12\pi F_\pi^4 \omega} + \frac{g_A^2 M_\pi^3 (-2M_\pi^2 + t + 2\omega^2)}{12\pi F_\pi^4 \omega} + \frac{t\omega}{2F_\pi^2 m} \right), \\
h^+ &= (c_3 - c_4) \left(\frac{ig_A^2 (\omega^2 - M_\pi^2)^{3/2}}{6\pi F_\pi^4 \omega} - \frac{g_A^2 M_\pi^3}{6\pi F_\pi^4 \omega} \right), \\
h^- &= c_4 \left(\frac{4g_A^2 \tilde{J}_0(\omega) (M_\pi^2 - \omega^2)}{3F_\pi^4 \omega} + \frac{-6(5g_A^2 + 1) M_\pi^2 + 8g_A^2 \omega^2 + t}{144\pi^2 F_\pi^4} + \frac{ig_A^2 (M_\pi^2 - \omega^2) \sqrt{\omega^2 - M_\pi^2}}{6\pi F_\pi^4 \omega} \right. \\
& \left. + \frac{\tilde{I}_{20}(t) (t - 4M_\pi^2)}{6F_\pi^4} + \frac{\omega}{F_\pi^2 m} \right) + \frac{\bar{e}_{17} (8M_\pi^2 - 4t)}{F_\pi^2} + \frac{8\bar{e}_{18} \omega^2}{F_\pi^2} + \frac{8(\bar{e}_{21} - \frac{\bar{e}_{37}}{2}) M_\pi^2}{F_\pi^2}. \tag{B.4}
\end{aligned}$$

The low-energy constants and the kinematical variables entering these expressions are defined in sections II, III and IV. The loop functions are defined via:

$$\begin{aligned}
\tilde{J}_0(\omega) &= \frac{\omega}{8\pi^2} - \frac{\sqrt{\omega^2 - M_\pi^2}}{4\pi^2} \log \left(\sqrt{\frac{\omega^2}{M_\pi^2} - 1} + \frac{\omega}{M_\pi} \right), \\
\tilde{K}_0(t) &= -\frac{1}{8\pi\sqrt{-t}} \arctan \frac{\sqrt{-t}}{2M_\pi},
\end{aligned}$$

$$\tilde{I}_{20}(t) = \frac{1}{16\pi^2} - \frac{\sqrt{1-4M_\pi^2/t}}{16\pi^2} \log \frac{\sqrt{1-4M_\pi^2/t} + 1}{\sqrt{1-4M_\pi^2/t} - 1}. \quad (\text{B.5})$$

-
- [1] N. Kalantar-Nayestanaki, E. Epelbaum, J. G. Messchendorp and A. Nogga, Rept. Prog. Phys. **75**, 016301 (2012) [arXiv:1108.1227 [nucl-th]].
 - [2] E. Epelbaum, H. -W. Hammer and U. -G. Meißner, Rev. Mod. Phys. **81**, 1773 (2009) [arXiv:0811.1338 [nucl-th]].
 - [3] R. Machleidt and D. R. Entem, Phys. Rept. **503**, 1 (2011) [arXiv:1105.2919 [nucl-th]].
 - [4] E. Epelbaum and U. -G. Meißner, arXiv:1201.2136 [nucl-th], to appear in Ann. Rev. Nucl. Part. Sci.
 - [5] D. R. Entem and R. Machleidt, Phys. Rev. C **68**, 041001 (2003) [nucl-th/0304018].
 - [6] E. Epelbaum, W. Glöckle and U. -G. Meißner, Nucl. Phys. A **747**, 362 (2005) [nucl-th/0405048].
 - [7] U. van Kolck, Phys. Rev. C **49**, 2932 (1994).
 - [8] E. Epelbaum, A. Nogga, W. Glöckle, H. Kamada, U. G. Meißner and H. Witala, Phys. Rev. C **66**, 064001 (2002) [nucl-th/0208023].
 - [9] W. Glöckle, H. Witala, D. Huber, H. Kamada and J. Golak, Phys. Rept. **274**, 107 (1996).
 - [10] Y. Koike and J. Haidenbauer, Nucl. Phys. A **463**, 365 (1987).
 - [11] H. Witala, D. Hüber and W. Glöckle, Phys. Rev. C **49** R14, (1999).
 - [12] C. Duweke, R. Emmerich, A. Imig, J. Ley, G. Tenckhoff, H. Paetz gen.Schieck, J. Golak and H. Witala *et al.*, Phys. Rev. C **71**, 054003 (2005) [nucl-ex/0412024].
 - [13] J. Ley, C. Duweke, R. Emmerich, A. Imig, H. P. g. .Schieck, J. Golak, H. Witala and E. Epelbaum *et al.*, Phys. Rev. C **73**, 064001 (2006).
 - [14] M. Viviani *et al.*, arXiv:1004.1306 [nucl-th].
 - [15] V. Bernard, E. Epelbaum, H. Krebs and U. -G. Meißner, Phys. Rev. C **77**, 064004 (2008) [arXiv:0712.1967 [nucl-th]].
 - [16] V. Bernard, E. Epelbaum, H. Krebs and U. -G. Meißner, Phys. Rev. C **84**, 054001 (2011) [arXiv:1108.3816 [nucl-th]].
 - [17] S. Ishikawa and M. R. Robilotta, Phys. Rev. C **76**, 014006 (2007) [arXiv:0704.0711 [nucl-th]].
 - [18] C. Ordonez, L. Ray and U. van Kolck, Phys. Rev. Lett. **72**, 1982 (1994).
 - [19] N. Kaiser, S. Gerstendorfer and W. Weise, Nucl. Phys. A **637**, 395 (1998) [nucl-th/9802071].
 - [20] H. Krebs, E. Epelbaum and U. -G. Meißner, Eur. Phys. J. A **32**, 127 (2007) [nucl-th/0703087].
 - [21] E. Epelbaum, H. Krebs and U. -G. Meißner, Nucl. Phys. A **806**, 65 (2008) [arXiv:0712.1969 [nucl-th]].
 - [22] E. Epelbaum, H. Krebs and U. -G. Meißner, Phys. Rev. C **77**, 034006 (2008) [arXiv:0801.1299 [nucl-th]].
 - [23] V. Bernard, N. Kaiser and U. -G. Meißner, Nucl. Phys. A **615**, 483 (1997) [hep-ph/9611253].
 - [24] N. Kaiser, R. Brockmann and W. Weise, Nucl. Phys. A **625**, 758 (1997) [nucl-th/9706045].
 - [25] R. Machleidt and D. R. Entem, J. Phys. G G **37**, 064041 (2010) [arXiv:1001.0966 [nucl-th]].
 - [26] S. C. Pieper, V. R. Pandharipande, R. B. Wiringa and J. Carlson, Phys. Rev. C **64**, 014001 (2001) [nucl-th/0102004].
 - [27] V. Bernard, N. Kaiser and U. -G. Meißner, Int. J. Mod. Phys. E **4**, 193 (1995) [hep-ph/9501384].
 - [28] N. Fettes, U. -G. Meißner, M. Mojzis and S. Steininger, Annals Phys. **283**, 273 (2000) [Erratum-ibid. **288**, 249 (2001)] [hep-ph/0001308].
 - [29] E. Epelbaum, U. -G. Meißner, J. E. Palomar, Phys. Rev. C **71**, 024001 (2005). [nucl-th/0407037].
 - [30] J. L. Friar, G. L. Payne, U. van Kolck, Phys. Rev. C **71**, 024003 (2005). [nucl-th/0408033].
 - [31] J. L. Friar, U. van Kolck, M. C. M. Rentmeester, R. G. E. Timmermans, Phys. Rev. C **70**, 044001 (2004). [nucl-th/0406026].
 - [32] N. Fettes, U.-G. Meißner and S. Steininger, Nucl. Phys. A **640**, 199 (1998) [arXiv:hep-ph/9803266].
 - [33] J. Gasser, M. A. Ivanov, E. Lipartia, M. Mojzis and A. Rusetsky, Eur. Phys. J. C **26**, 13 (2002) [hep-ph/0206068].
 - [34] J. L. Friar, D. Huber and U. van Kolck, Phys. Rev. C **59**, 53 (1999) [nucl-th/9809065].
 - [35] J. L. Friar and S. A. Coon, Phys. Rev. C **49**, 1272 (1994).
 - [36] E. Epelbaum, W. Glöckle and U. -G. Meißner, Nucl. Phys. A **637**, 107 (1998) [nucl-th/9801064].
 - [37] E. Epelbaum, U. -G. Meißner and W. Glöckle, Nucl. Phys. A **714**, 535 (2003) [nucl-th/0207089].
 - [38] E. Epelbaum, Phys. Lett. B **639**, 456 (2006) [nucl-th/0511025].
 - [39] E. Epelbaum, Eur. Phys. J. A **34**, 197 (2007) [arXiv:0710.4250 [nucl-th]].
 - [40] S. Kolling, E. Epelbaum, H. Krebs and U. -G. Meißner, Phys. Rev. C **80**, 045502 (2009) [arXiv:0907.3437 [nucl-th]].
 - [41] S. Kolling, E. Epelbaum, H. Krebs and U. -G. Meißner, Phys. Rev. C **84**, 054008 (2011) [arXiv:1107.0602 [nucl-th]].
 - [42] J. Gasser, H. Leutwyler, Annals Phys. **158**, 142 (1984).
 - [43] G. Ecker and M. Mojžiš, Phys. Lett. B **365**, 312 (1996) [arXiv:hep-ph/9508204].
 - [44] T. Becher and H. Leutwyler, JHEP **0106**, 017 (2001) [hep-ph/0103263].
 - [45] N. Fettes and U. -G. Meißner, Nucl. Phys. A **676**, 311 (2000) [hep-ph/0002162].
 - [46] N. Fettes and U. -G. Meißner, Nucl. Phys. A **693**, 693 (2001) [hep-ph/0101030].
 - [47] J. M. Alarcon, J. Martin Camalich, J. A. Oller and L. Alvarez-Ruso, Phys. Rev. C **83**, 055205 (2011) [arXiv:1102.1537 [nucl-th]].
 - [48] K. Torikoshi and P. J. Ellis, Phys. Rev. C **67**, 015208 (2003) [nucl-th/0208049].
 - [49] A. Gasparyan and M. F. M. Lutz, Nucl. Phys. A **848**, 126 (2010) [arXiv:1003.3426 [hep-ph]].
 - [50] V. Bernard, Prog. Part. Nucl. Phys. **60**, 82 (2008) [arXiv:0706.0312 [hep-ph]].

- [51] S. Weinberg, Nucl. Phys. B **363**, 3 (1991).
- [52] E. Epelbaum, Prog. Part. Nucl. Phys. **57**, 654 (2006) [nucl-th/0509032].
- [53] R. G. E. Timmermans, T. A. Rijken and J. J. de Swart, Phys. Rev. Lett. **67**, 1074 (1991).
- [54] V. Baru, C. Hanhart, M. Hoferichter, B. Kubis, A. Nogga and D. R. Phillips, Phys. Lett. B **694**, 473 (2011) [arXiv:1003.4444 [nucl-th]].
- [55] J. Gasser and U. G. Meißner, Phys. Lett. B **258**, 219 (1991).
- [56] R. A. Arndt, W. J. Briscoe, I. I. Strakovsky and R. L. Workman, Phys. Rev. C **74**, 045205 (2006) [nucl-th/0605082].
- [57] R. Koch, Nucl. Phys. A **448**, 707 (1986).
- [58] P. Buettiker and U. -G. Meißner, Nucl. Phys. A **668**, 97 (2000) [hep-ph/9908247].
- [59] M. C. M. Rentmeester, R. G. E. Timmermans and J. J. de Swart, Phys. Rev. C **67**, 044001 (2003) [nucl-th/0302080].